Journal of Molecular Graphics and Modelling 34 (2012) 89–100

Contents lists available at SciVerse ScienceDirect

Journal of Molecular Graphics and Modelling

journal homepage: www.elsevier.com/locate/JMGM

Virtual screening filters for the design of type II p38 MAP kinase inhibitors: A fragment based library generation approach

Preethi Badrinarayan, G. Narahari Sastry*

Molecular Modeling Group, Organic Chemical Sciences, Indian Institute of Chemical Technology, Tarnaka, Hyderabad 500607, India

ARTICLE INFO

Article history:
Received 21 September 2011
Received in revised form
19 November 2011
Accepted 27 December 2011
Available online 3 January 2012

Keywords:
Kinase
p38 MAP
Specificity
Virtual screening filters
Fragment based drug design

ABSTRACT

In this work, we introduce the development and application of a three-step scoring and filtering procedure for the design of type II p38 MAP kinase leads using allosteric fragments extracted from virtual screening hits. The design of the virtual screening filters is based on a thorough evaluation of docking methods, DFG-loop conformation, binding interactions and chemotype specificity of the 138 p38 MAP kinase inhibitors from Protein Data Bank bound to DFG-in and DFG-out conformations using Glide, GOLD and CDOCKER. A 40 ns molecular dynamics simulation with the apo, type I with DFG-in and type II with DFG-out forms was carried out to delineate the effects of structural variations on inhibitor binding. The designed docking-score and sub-structure filters were first tested on a dataset of 249 potent p38 MAP kinase inhibitors from seven diverse series and 18,842 kinase inhibitors from PDB, to gauge their capacity to discriminate between kinase and non-kinase inhibitors and likewise to selectively filter-in target-specific inhibitors. The designed filters were then applied in the virtual screening of a database of ten million (10^7) compounds resulting in the identification of 100 hits. Based on their binding modes, 98 allosteric fragments were extracted from the hits and a fragment library was generated. New type II p38 MAP kinase leads were designed by tailoring the existing type I ATP site binders with allosteric fragments using a common urea linker. Target specific virtual screening filters can thus be easily developed for other kinases based on this strategy to retrieve target selective compounds.

1. Introduction

The involvement of kinases in a wide range of disease conditions from inflammation to oncogenesis makes them pharmaceutically important druggable targets for therapeutic intervention [1,2]. Majority of kinase drugs are type I inhibitors which target the catalytic ATP binding site but due to the high level of similarity within the ATP binding sites of protein kinases, it is often difficult to achieve the required pharmacological selectivity. However, each kinase has unique structural motifs, protein–protein interaction segments, specific dynamic properties, and allosteric binding site which distinguish them from each other [3–5]. This uniqueness of a protein kinase can be exploited pharmaceutically to create specificity. A number of strategies targeting different aspects of kinases like size of gatekeeper residue [6], metabolic properties of the target involved in signal transduction [7], protonation switch in drug binding [8], network analysis and fingerprint of structure and sequence of kinome [9], recognition properties affecting selectivity [10], fragment based drug design (FBDD) [11] have been employed. Most of the kinase inhibitors developed to date bind to the ATP binding site when the kinase is in its active conformation, but targeting the inactive conformations is currently being explored as a strategy for the design of more selective kinase inhibitors. Design of type II inhibitors which exploit the conserved ATP site as well as the non-conserved allosteric site of the inactive kinase conformation is a desirable option. Type II inhibitors bind to the inactive DFG-out conformation of the kinase caused due to the conformational transition of the DFG-loop. This opens up the second hydrophobic pocket referred to as the allosteric site in the current study. The DFG-loop formed by the catalytic amino acid triad Asp, Phe and Glu is found at the anterior end of activation loop and is a common feature in kinases. A number of studies have demonstrated the advantages of targeting the DFG-out binding mode of kinases in general and p38 MAP kinase (p38 MAPK) in particular [12]. The kinase inhibitors are governed by an integrated interaction-network with major motifs like hinge, conserved residues, DFG-loop, water, aromatic residues, etc. The patterns of interactions are conserved for a particular class of inhibitors and play a key role in rendering specificity [13].

Previous studies construe that a given fragment has a tendency to occupy the same part of the binding site irrespective of its position in the parent scaffold. Thus, the final inhibitor adopts

* Corresponding author. Tel.: +91 40 2719 3016.
E-mail addresses: gnsastry@gmail.com, gnsastry@iict.res.in (G.N. Sastry).

1093-3263/$ – see front matter © 2012 Elsevier Inc. All rights reserved.
doi:10.1016/j.jmgm.2011.12.009

the same binding mode as the original fragment hit and reiterates similar pattern of interactions [14]. The abundant structural information obtained from crystal structures of proteins and their various inhibitors facilitate fragment-based lead discovery leads [15]. Considering the availability of a large number of type I ATP site inhibitors with good efficacy but less specificity, the redesigning of these existing type I inhibitors into type II to bring in specificity is a promising approach. In the current study, we put forth the development and application of target specific virtual screening filters to identify allosteric fragments for the design of type II p38 MAP kinase leads. Allosteric site inhibitors are less in number as compared to the ATP site binders therefore virtual screening of a database of 10^7 compounds was undertaken to identify more number of diverse allosteric fragments. Virtual screening is an important and favorable tool for the identification of leads [16,17]. However, considering the increase in chemical space and availability of a spectrum of screening techniques, choice of the right screening tool and filter is necessary to identify potential leads in minimum time and with maximum precision [18]. Many reports have been published which describe different docking algorithms and scoring functions for virtual screening [19], compare and contrast two or more programs [20] or probe into deeper issues like unbiased construction of benchmarks [21,22], ensemble docking [23], induced-fit effects [24], multi-step strategies [25], etc. However, none of them have tried to decipher the influence of kinase DFG-loop transition and chemotype specificity on docking. Therefore, an evaluation of the performance of docking protocols for the twin DFG-conformations was carried out as a prelude to the design of filters. A 40 ns molecular dynamics simulation with different conformations of p38 MAPK was carried out to delineate the effects of structural variations on inhibitor binding.

Filters were designed based on the DFG-loop conformation, binding interactions and chemotype specificity. The first filter is based on the score components of the two docking protocols used in the study and the other on the sub-structure interactions. Both the filters were tested on a dataset of 249 potent p38 MAP kinase inhibitors from seven diverse series and 18,842 kinase inhibitors from PDB, to measure their capacity to discriminate between kinase and non-kinase inhibitors and also to selectively filter-in target-specific inhibitors. These filters were then used in virtual screening to identify potential hits from which a library of p38 MAPK specific allosteric fragments was extracted. New type II p38 MAPK leads were designed by merging the existing type I ATP site binders and the identified allosteric fragments with a common linker. Modelling and lead design studies are an important step in the screening and design of leads [26–32]. Target specific virtual screening filters can thus be easily developed for other kinases based on this strategy and applied to retrieve target selective compounds for the fragment based design of type II kinase leads.

2. Methods

2.1. Dataset

Four major datasets have been used in the current study at different stages. The first dataset comprising of p38 MAPK inhibitors and drugs from Protein Data Bank (PDB) was used for the evaluation of docking protocols and design of filters. The second dataset containing the diverse p38 MAPK and the third dataset containing kinase inhibitors from PDB were used for testing the designed virtual screening filters and the fourth dataset consisting 10^7 compounds was used for virtual screening. To prepare the first dataset, the available 98 p38 MAPK crystal structures were downloaded from PDB [33] and 138 co-crystals were extracted and docked onto their respective receptors to study their binding modes, interactions and chemotype preferences. The crystal structures were clustered into DFG-in (50), DFG-out (45) and outliers (43) based on the position of DFG-loop conformation especially F169. The co-crystal binding to a site other than ATP or allosteric site was termed as an outlier. For the second set, seven diverse series of 249 p38 MAPK inhibitors with good efficacy and comprising of DFG-in (143), DFG-out (82) and dual conformation binders (24) were selected [34–40] and mixed with 10,000 non-kinase inhibitors. The third dataset constitutes the 18,842 kinase inhibitors present in Protein Data Bank. The fourth dataset of 10^7 compounds used for virtual screening was prepared from ZINC [41], GDB [42], Analyticon [43] and some in-house compounds. Fingerprints were generated for these compounds using Discovery Studio 2.1. A filter criterion based on Lipinski's rule of five was applied to the dataset to compile the final screening dataset [44].

2.2. Docking

The 98 p38 MAPK co-crystal complexes from PDB along with the three datasets were subjected to protein and ligand preparation. Prime and Modeller 9v5 were used for side-chain refinement and to build breaks present in the structures of p38 MAPK crystal structures downloaded from PDB [45,46]. The template sequence was selected based on the source target sequence from among the seven representative sets of p38 MAPK sequences in PDB and DFG-loop conformation (Table S1a). The quality of the constructed model was cross validated with Ramchandran plot (RAMPAGE) [47], energy profiles with ProSA [48] and the secondary structure was determined with STRIDE [49]. Two different program packages, Sybyl 6.9 [50] and Schrodinger [51] have been used for the purpose of molecule preparation, active site search and docking. Sybyl 6.9 was used in the preparation of inputs for proteins and ligand used for GOLD [52] and CDOCKER [53] docking. All the ligands were built and minimized using Tripos force field, MMFF94 atomic partial charges, implementing Powell's conjugate gradient method with a distance dependent dielectric constant, until a convergence gradient of 0.02 kcal/mol was accomplished. For GOLD protein preparation, all hydrogen were added using the Biopolymer module of Sybyl package and inhibitors within the active site, heteroatoms and all waters were removed. Proteins were minimized applying Kollman's all partial atomic charges, Powell's conjugate gradient method with distance dependent dielectric constant value of 1.0 kcal/mol and a gradient convergence value of 0.05 kcal/mol. While for Glide, protein preparation wizard was used to prepare the proteins after adding hydrogen. The side-chain residues were refined using Prime. Ligands were submitted to the LigPrep module to generate a range of ionization states populated at a given pH range of 7.4 ± 2 followed by an exhaustive conformational sampling with Confgen [54].

The rigid docking protocols of GOLD 3.2, Glide 4.5 and CDOCKER 2.1 have been employed. The two options of docking namely standard precision (SP) and extra precision (XP) of 'Glide' module were used for Glide docking. The grid was generated by specifying M109 residue as grid centre. The default SP docking settings were used and the conformations obtained from SP were used as input for XP. Docking with GOLD and CDOCKER was done using the default parameters. Hydrophobic and hydrophilic maps were generated to get an idea of the solvent accessible regions. Every time, ten poses were generated for each docked molecule.

2.3. Molecular dynamics simulations

All MD simulations were performed by using the parallel MD program Desmond [55]. The complexes were prepared with protein-preparation wizard. The OPLS 2005 force field was used to model all peptide interactions, and an orthorhombic

water-box of 10 Å with TIP3P model was used for water [56]. All MD simulations were at constant pressure (1 bar), maintained using a Berendsen barostat, and constant temperature (300 K) maintained using Berendsen thermostats. The pressure and temperature control used a relaxation time of 0.5 ps. All simulations used a RESPA integrator with a 2.0 fs time step for the bonded, van der Waals and short-range Coulomb interactions, and a 6.0 fs time step for the long-range Coulomb interactions. The system was equilibrated with the default protocol employed in Desmond, which consists of a series of restrained minimizations and MD simulations designed to slowly relax the system without substantial deviation from the initial protein co-ordinates. A 40 ns NPT simulation was carried out recording frames at an interval of 1.2 ps. The simulated complexes are: (a) apo-protein (PDB 1WFC); (b) type I inhibitor bound to DFG-in conformation (PDB 1A9U); (c) type II inhibitor bound to DFG-out (PDB 1KV2); (d) two top ranking designed inhibitors B96 and A71 bound to DFG-out conformation.

2.4. Strategy

The fragment based lead design strategy proposed in the current study addresses four important issues. First, the evaluation factors governing the performance tools for the two DFG-conformations. The second issue compares and contrasts the binding modes, interactions and chemotype specificity of inhibitors with the twin DFG-conformations in order to design reliable target specific virtual screening filters. The third issue delineates the development of target-specific filters and virtual screening to identify allosteric fragments. The fourth and most important issue is the generation of the allosteric fragment library followed by the design of leads.

3. Evaluation of different docking protocols for p38 Map kinase

The design of leads for a particular drug target invokes meticulous study of the target, existing inhibitors and the tools used [19–21]. Evaluation of docking methods is therefore necessary to measure the capacity of most of these protocols to identify the correct binding pose and appropriately rank the pose having lowest RMSD difference with the co-crystal pose as the best scoring pose. Docking plays a pivotal role in the current study as it is the basic protocol used to decipher the DFG-loop conformation, binding interactions and chemotype specificity which were used in the design of filters. In concurrence with this idea, three docking protocols viz., GOLD, Glide and CDOCKER were evaluated with the first dataset of 138 p38 MAPK co-crystal complexes (Table S1). Ten poses were generated for each of the 138 co-crystal complex with all the three docking protocols, summing up to a total of 4140 pose which were used for evaluation. An analysis of the performance of the docking tools in terms of RMSD, score, DFG-loop conformation and chemotype specificity has been given in the current section.

Docking accuracy is considered high if the RMSD between the docked and co-crystal pose is less. Majority of the lowest RMSD poses in Glide 95.65% fall within 2 Å closely followed by GOLD 94.20% and CDOCKER 71.74% (Table S2a). Similar patterns are observed in RMSD threshold at smaller intervals. On analysis of the docked poses it was observed that 89.86, 81.84 and 50.72% best scoring poses (BSP) of GLIDE, GOLD and CDOCKER respectively lie within a cut-off of 2 Å RMSD (Fig. S1a). High RMSD is found in cases where modelling of breaks and side-chain refinement of receptor especially near the DFG-loop were inadequate to capture the induced-fit effect caused by the bound co-crystal. This caused slight conformational changes in the active site as a result of which higher variation in the binding mode as compared to the co-crystal pose is observed. The structure of ligand is also seen to play a major role, as with the increase in the number of rotatable bonds of ligand more number of conformers are generated giving a widespread range of input which score well but do not resemble the co-crystal pose (Table S2b).

Ranking of the scored solutions in relation to RMSD was investigated to correlate score-based ranks with RMSD (Table S3). Although Glide fared better in obtaining low RMSD poses, GOLD proved efficient in ranking. The number of best scored (RANK1) poses being the lowest RMSD pose is comparatively high in GOLD as compared to Glide and CDOCKER. This inspired a detailed analysis of the individual scoring components of Glide and GOLD (Fig. S1b). Ten best scored poses for each of the 138 co-crystals generated from both Glide and GOLD summing up to a total of 2760 poses were studied in terms of score and RMSD to delineate the non-complementarities between the score and RMSD. Highest RMSD pose score is observed to be better than the lowest RMSD score in cases where the score is high due to the contribution of H-bond interactions which contribute to the scoring component in a major fashion. Lack of H-bond formation led to a lower score due to which poses having low RMSD (close to the co-crystal pose) scored less. Such instances occurred when a conformer having high RMSD difference in comparison to the co-crystal was docked. In contrast, when H-bonds pattern match that of the co-crystal pose, best score pose is the lowest RMSD pose. It is also seen in cases where the lowest RMSD conformer forms a part of the best scoring pose (Fig. S2).

4. DFG-loop conformation and chemotype specificity

The 98 p38 MAPK crystal structures with 138 bound inhibitors comprise of seven different sequences which belong to different origin and sub-families (Table S1a). 86 of these are from *Homo sapiens* (p38α, p38β, p38δ, MAPK2) while 11 are from *Mus musculus* (Mapk14, MEF2A, MKK3b) and one chimera containing chains from both *H. sapiens* and *M. musculus* (Table S4). The activation loop in majority of the crystal structures is not phosphorylated. The DFG-loop in these crystal structures is observed to be in different conformations. The hydrophobic allosteric pocket is less accessible in the DFG-in conformation as compared to the adjacent ATP pocket. Thus the inhibitors binding to the DFG-in and DFG-out conformations vary in size and nature (Fig. 1). Accordingly an analysis of the docked poses of all the co-crystal complexes was carried out demarcating the occupancy and nature of inhibitors to bind to these two DFG-conformations (Tables S5 and S6). The residue numbers of p38α isoform are used henceforth in discussion.

Majority of the DFG-in binders occupy both DFG-in and DFG-out active sites well. Their scores are higher on binding with the DFG-out active site due to interactions with D168 and F169 exposed only in the inactive conformation (Table S7). The bulky allosteric group of the DFG-out binders forms H-bond and close contacts with the hydrophobic pocket opened on transition of the DFG-loop. But when these compounds are docked to DFG-in receptor, the allosteric part of the inhibitor clashes with F169 of the DFG-in active site thus asserting pressure on the adjacent polar sugar-pocket residues, apolar hinge residues of adenine sub-pocket M109, G110, T106 present at the extreme ends, highly flexible Y35 and the conserved salt-bridge former K53 (Table S8). The ATP site binders display a conserved set of H-bonds with hinge region residues. The type II inhibitors exhibit more number of lipophilic interactions with the hydrophobic allosteric site to overcome the energetic penalty incurred on adopting the DFG-out conformation. Comparison of the docking scores of the two DFG-conformations reveal major difference among the van der Waals components and minor differences in the columbic and lipophilic score components.

MD simulations of 40 ns each were done to further compare and contrast the structural variations and molecular recognition

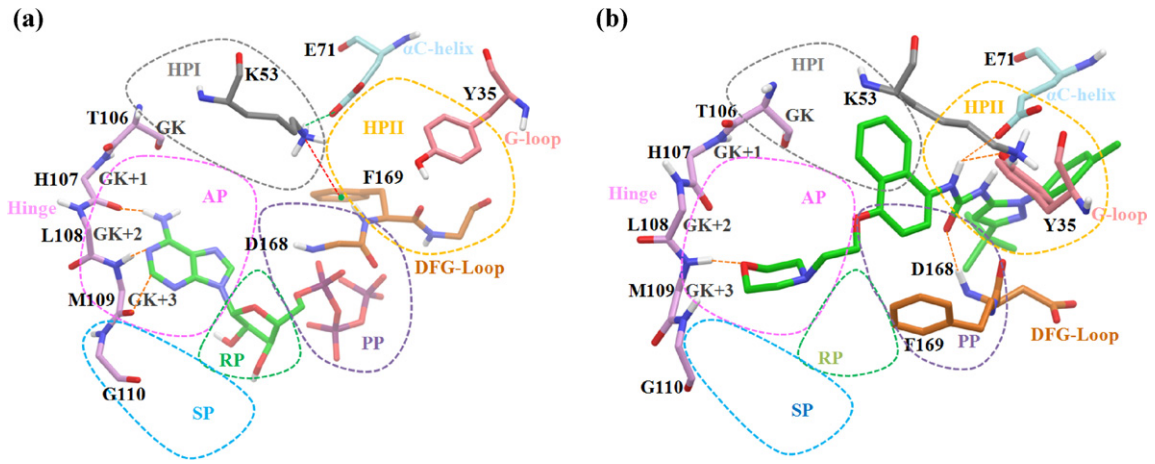

Fig. 1. The figure illustrates the features of (a) DFG-in (PDB code: 1A9U docked with ATP) versus (b) DFG-out (PDB code: 1KV2) binding. The six kinase sub-pockets viz., adenine (AP), ribose (RP), phosphate (PP), solvent (SP), back (HPI) and hydrophobic allosteric (HPII) have also been delineated.

properties of p38 MAP kinase in the apo, DFG-in and DFG-out forms bound to type I and type II inhibitors (Fig. 2). The conformational space scaled during the 40 ns MD simulation when dissected based on major interaction motifs delineates fluctuations in the time-scale around 8.5 and 24.0 ns onwards for apo-protein which shows the tendency of the DFG-loop to transit from its parent position. The type I inhibitor is seen to bind tightly with the hinge in DFG-in conformation (Fig. S3a). The protein in general and DFG-loop in particular displays less number of varied conformations as initially but from 32 ns, the side chain of F169 is seen to drift slowly towards an intermediate position between DFG-in and DFG-out. The DFG-out conformation with the type II inhibitor shows a constant rising trend from 4.0 ns delineating several pseudo DFG-out conformations (Fig. S3b). The RMSD of protein heavy atoms, backbone and Cα of the simulated complex in relation to the initial docked structure shows an average trend, in the ranges of 0.940–3.132, 0.836–2.986, 0.774–3.452 Å respectively for all the complexes (Fig. S4). Inspection of crystal structures reveal that in case of type II inhibitors which interact with the DFG-motif, the activation loop is not phosphorylated. The binding modes of inhibitor delineate the tendency of a particular chemotype to occupy same region of the active site irrespective of the scaffold it constitutes displaying similar pattern of interactions. These observations were incorporated in the strategy developed for the design of leads.

5. Virtual screening filters

Virtual screening filters are designed based on evaluation of docking protocols, DFG-loop conformation and chemotype specificity studies carried out in the previous sections. They have been developed to filter out docked compounds on basis of their binding affinity and interactions. The logic behind designing such filters is that existing p38 MAPK co-crystals represent a diverse series of DFG-in and DFG-out binders. In addition, with the observation that a chemotype binding to a particular region of active site reiterates similar pattern of interactions, a potential hit should fall in the scoring range of its counterparts. Therefore, two filters based on docking score-components and sub-structure interactions were identified and used as filters.

Consensus scoring using different scoring functions based on different docking algorithms is a viable resort to drop out false positives [57]. Therefore, the score components of two docking protocols GOLD and Glide were used in the design of docking-score filters. The 138 p38 MAPK co-crystals were docked with both GOLD and Glide and ten poses for each of the co-crystal were saved. These 2760 poses (138 × 2GOLD + Glide × 10) were used as a starting point (Tables S5a and S6a). The scoring components of the best scoring pose among the ten poses were retained for each co-crystal (Tables S5b and S6b). The score components of the 276 best scoring

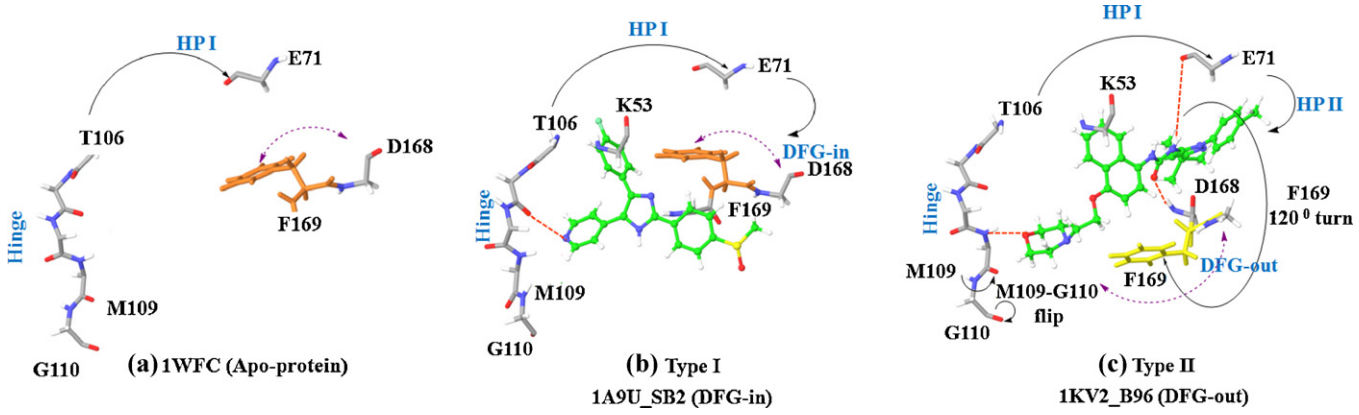

Fig. 2. Model systems used to study the structural variations and its relative effect on inhibitor binding as observed in a molecular dynamics simulation of 40 ns with (a) apo (b) type I bound to DFG-in and (c) type II bound to DFG-out conformations of p38 MAP kinase.

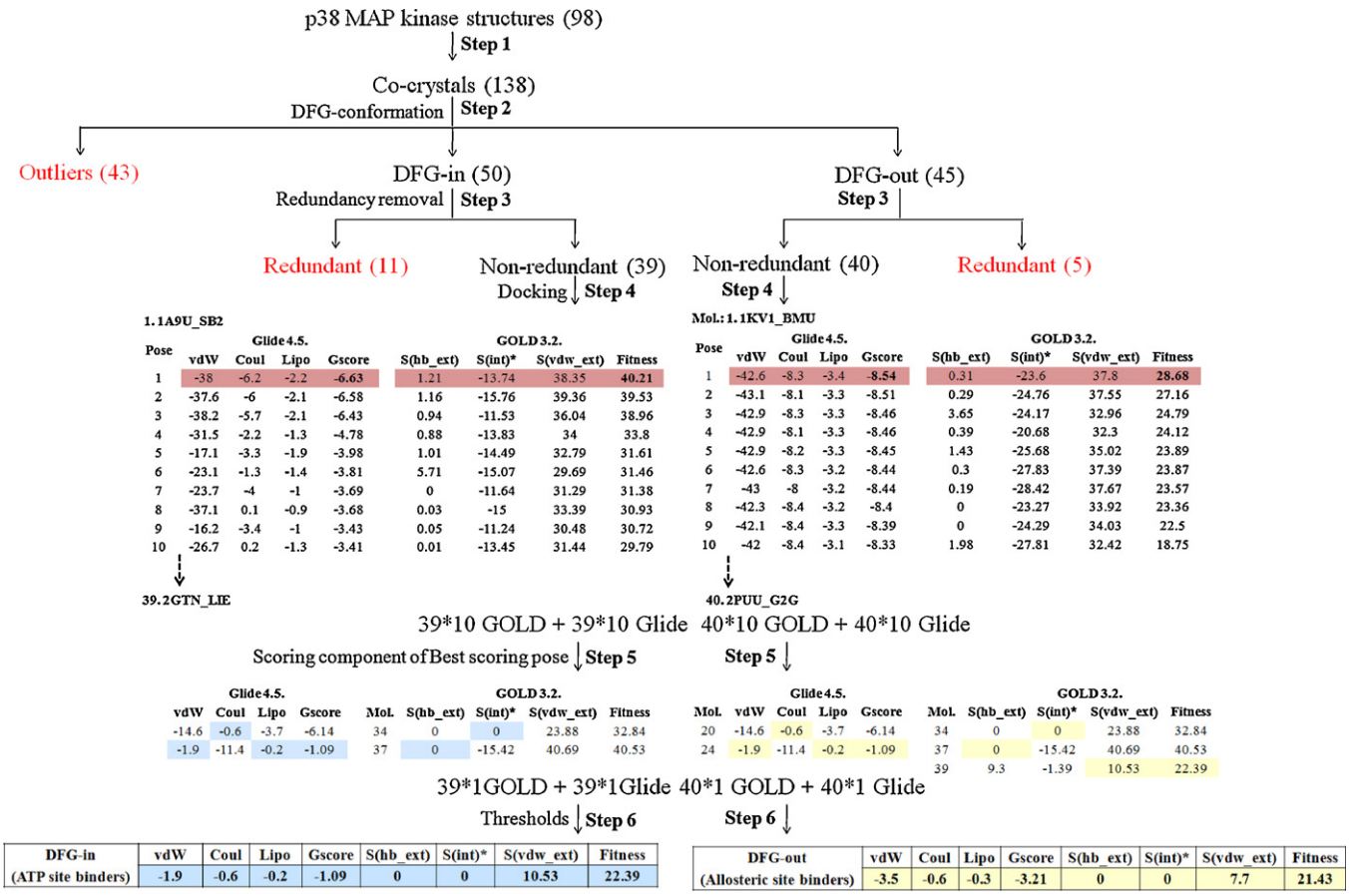

Pose	Glide 4.5. vdW	Coul	Lipo	Gscore	GOLD 3.2. S(hb_ext)	S(int)*	S(vdw_ext)	Fitness
1	-38	-6.2	-2.2	-6.63	1.21	-13.74	38.35	40.21
2	-37.6	-6	-2.1	-6.58	1.16	-15.76	39.36	39.53
3	-38.2	-5.7	-2.1	-6.43	0.94	-11.53	36.04	38.96
4	-31.5	-2.2	-1.3	-4.78	0.88	-13.83	34	33.8
5	-17.1	-3.3	-1.9	-3.98	1.01	-14.49	32.79	31.61
6	-23.1	-1.3	-1.4	-3.81	5.71	-15.07	29.69	31.46
7	-23.7	-4	-1	-3.69	0	-11.64	31.29	31.38
8	-37.1	0.1	-0.9	-3.68	0.03	-15	33.39	30.93
9	-16.2	-3.4	-1	-3.43	0.05	-11.24	30.48	30.72
10	-26.7	0.2	-1.3	-3.41	0.01	-13.45	31.44	29.79

Pose	Glide 4.5. vdW	Coul	Lipo	Gscore	GOLD 3.2. S(hb_ext)	S(int)*	S(vdw_ext)	Fitness
1	-42.6	-8.3	-3.4	-8.54	0.31	-23.6	37.8	28.68
2	-43.1	-8.1	-3.3	-8.51	0.29	-24.76	37.55	27.16
3	-42.9	-8.3	-3.3	-8.46	3.65	-24.17	32.96	24.79
4	-42.9	-8.1	-3.3	-8.46	0.39	-20.68	32.3	24.12
5	-42.9	-8.2	-3.3	-8.45	1.43	-25.68	35.02	23.89
6	-42.6	-8.3	-3.2	-8.44	0.3	-27.83	37.39	23.87
7	-43	-8	-3.2	-8.44	0.19	-28.42	37.67	23.57
8	-42.3	-8.4	-3.2	-8.4	0	-23.27	33.92	23.36
9	-42.1	-8.4	-3.3	-8.39	0	-24.29	34.03	22.5
10	-42	-8.4	-3.1	-8.33	1.98	-27.81	32.42	18.75

Glide 4.5. vdW	Coul	Lipo	Gscore	Mol.	GOLD 3.2. S(hb_ext)	S(int)*	S(vdw_ext)	Fitness
-14.6	-0.6	-3.7	-6.14	34	0	0	23.88	32.84
-1.9	-11.4	-0.2	-1.09	37	0	-15.42	40.69	40.53

Glide 4.5. vdW	Coul	Lipo	Gscore	Mol.	GOLD 3.2. S(hb_ext)	S(int)*	S(vdw_ext)	Fitness
-14.6	-0.6	-3.7	-6.14	20	0	0	23.88	32.84
-1.9	-11.4	-0.2	-1.09	24	0	-15.42	40.69	40.53
				39	9.3	-1.39	10.53	22.39

DFG-in (ATP site binders)	vdW	Coul	Lipo	Gscore	S(hb_ext)	S(int)*	S(vdw_ext)	Fitness
	-1.9	-0.6	-0.2	-1.09	0	0	10.53	22.39

DFG-out (Allosteric site binders)	vdW	Coul	Lipo	Gscore	S(hb_ext)	S(int)*	S(vdw_ext)	Fitness
	-3.5	-0.6	-0.3	-3.21	0	0	7.7	21.43

Fig. 3. Schematic representation of the protocol followed for the design of target and DFG-conformation specific docking filters for virtual screening using scoring components of GOLD and Glide obtained on docking p38 MAPK inhibitors. The 138 co-crystals were extracted from the 98 p38 MAPK crystal structures from PDB and classified on the basis of their DFG-loop conformation. Redundant inhibitors were removed and the non-redundant DFG-in (39) and DFG-out (40) were docked with GOLD and Glide generating 10 poses for each co-crystal*. The scoring component of the best score pose among the ten poses was selected for each of the DFG-in and DFG-out inhibitors*. The lowest value of each scoring component of GOLD and Glide among the best score poses for both DFG-in and DFG-out were selected as threshold for their respective class** 16 thresholds, 8 each for DFG-in and DFG-out thus formed the docking filters. *The scoring components of all the ten poses for each of the inhibitors is given in Tables S5a and S6a. **The scoring components of the best score pose for each of the inhibitors is given in Table S9 along with the lowest value of each scoring component for each class of inhibitors.

pose (138 × 2GOLD + Glide × 1) were clustered into two categories DFG-in and DFG-out based on the two DFG-loop conformation of the receptor to which the co-crystal was bound (Tables S7 and S8). The lowest value of each scoring component of the two docking protocols for each of the DFG-conformations was chosen as threshold (Table S9). Thus, 16 thresholds were identified comprising 8 score components four each from GOLD and Glide for DFG-in and DFG-out conformations (Fig. 3).

Conserved set of interactions between a set of protein-inhibitor complexes has been proved to be a useful tool to understand potency and selectivity of kinase inhibitors [58]. This information can be effectively used to define target constraints to assist virtual screening [59]. In an attempt to identify sub-structure interactions with different active-site regions, the 138 p38 MAPK inhibitors were first clustered on the basis of DFG-conformation which gave two subsets of 50 DFG-in, 45 DFG-out and 43 outliers (Fig. 4). The outliers were discarded and the two subsets were further segregated on the basis of their H-bond binding interactions (Fig. S5). Non-interacting sub-structures were discarded retaining only the 43 DFG-in and 23 DFG-out interacting sub-structures. Each of these two sets of interacting sub-structures were segregated into five clusters on the basis of similarity using maximum dissimilarity algorithm to mark out the diverse sub-structures. Cluster centres representing each cluster were identified. These 10 representative sub-structures, 5 each for DFG-in and DFG-out conformations were prioritized and used as sub-structure filters (Fig. 5). These sub-structures can thus be used as target-specific filters in different formats such as shape, SMILES or interaction-fingerprints for p38 MAP kinase virtual screening, to identify specific hits with maximum precision in minimum time.

5.1. Evaluation of filters

The designed filters were tested on two datasets, one comprising diverse p38 MAPK inhibitors with good efficacy mixed with non-kinase inhibitors in order to evaluate the capacity of the filters to differentiate between kinase and non-kinase inhibitors. The next testing was done exclusively on a set of kinase inhibitors to measure the capacity of the filters to selectively identify target specific p38 MAPK inhibitors even in the presence of structurally similar kinase inhibitors. Based on the study of p38 MAPK crystal structures, 1A9U (DFG-in) and 1KV2 (DFG-out) were chosen as representative receptors. Both the test sets were docked with both GOLD and Glide, generating ten pose for each docked molecule. A molecule was considered as predicted active for p38 MAPK if the 16 scoring values of the docked molecule were superior to the 16 thresholds (Table 1). All 249 p38 MAPK inhibitors in the second dataset followed the threshold developed for DFG-in and DFG-out inhibitors except seven in Glide docking (Fig. S6 and Tables S10 and S11). This exercise demonstrates the capacity of the filters to filter-in the diverse p38 MAP kinase inhibitors and throw out the non-kinase inhibitors. For the next test, the third dataset containing

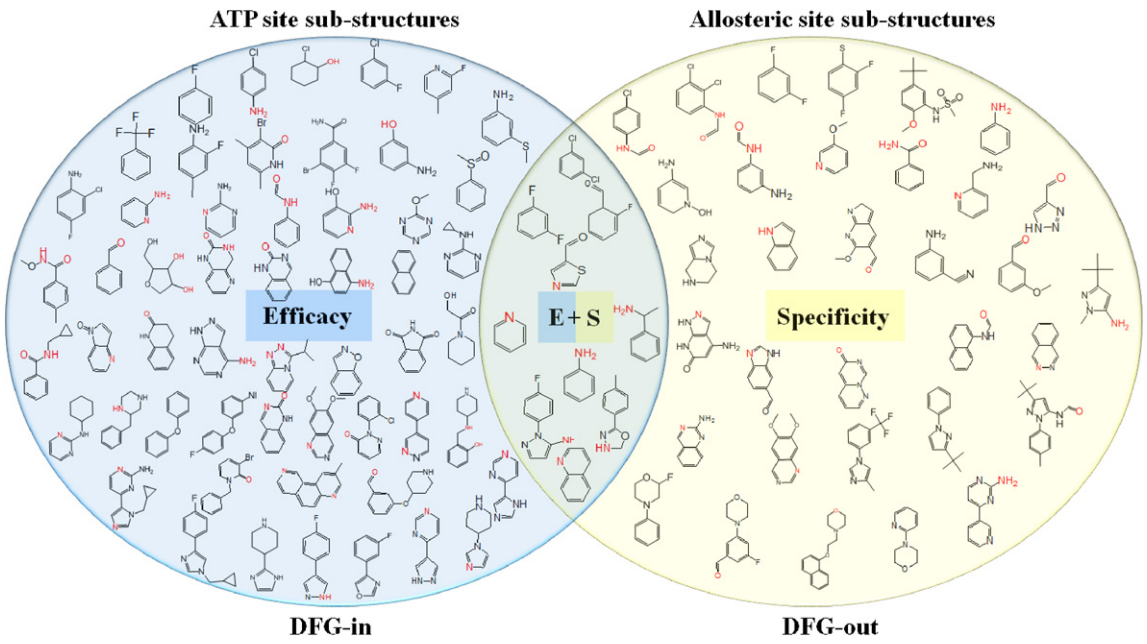

Fig. 4. Venn diagram representing the sub-structures of p38 MAP kinase DFG-in and DFG-out conformation binders from Protein Data Bank. The interacting atoms are shown in red. Each individual inhibitor is divided into sub-structures on basis of chemotype and preference obtained from docking. The ATP site sub-structures are shown in blue whereas the allosteric sub-structures are represented in pink. The sub-structures binding to other sites have been termed as outliers. The figure illustrates the increase in efficacy with ATP site binders and specificity with allosteric site binders. (For interpretation of the references to color in this figure legend, the reader is referred to the web version of this article.)

kinase inhibitors were segregated into 10 clusters based on similarity and 1693 non-redundant ones were used for testing (Table S12). The filters filtered out all non-p38 MAPK inhibitors except 38. On analysis, it was observed that out of the 38 outliers, 26 bind to target kinases which share very high sequence similarity with p38 MAPK (Table S13a). The sequence analysis, multiple sequence alignment and phylogenetic relationship with BLAST [60], ClustalW [61] and PHYLIP [62] are in agreement with the above observation. The 12 outliers which do not share sequence similarity were found to be co-crystallized to more number of kinases including p38 MAPK (Table S13b). Thus, the filters have proved to be efficient in filtering out 1667 (98.5%) non-p38 MAPK inhibitors, demonstrating their ability to selectively identify target-specific compounds.

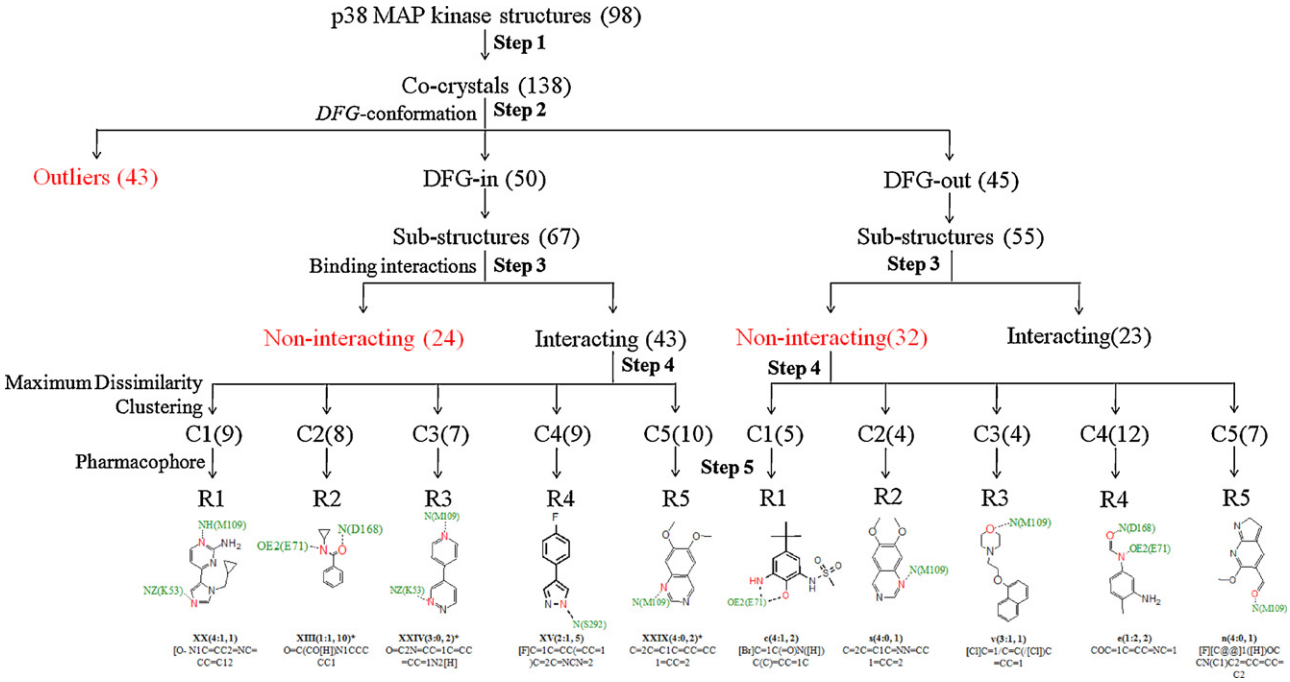

Fig. 5. Flow-chart depicting the design of sub-structure filters for p38 MAP kinase from its 138 inhibitors and 31 drugs. Step 1: extraction of bound ligands; Step 2: segregation of inhibitors based on the DFG-conformation of receptor; Step 3: separation of sub-structures on the basis of their interactions with active site region as obtained from docking; Step 4: clustering of the interacting sub-structures into 5, clusters with each cluster containing similar ligands; Step 5: selection of a representative structure/pharmacophore from each cluster giving 10 representative structure filters.

Table 1
Analysis of Glide 4.3 and GOLD 3.2 docking scores with similar and diverse datasets of p38 MAP kinase used for testing docking filters.

	Dataset	Receptor-DFG-in 1A9U		Receptor-DFG-out 1KV2	
		Highest	Lowest	Highest	Lowest
Glide	DFG-in *binders*	−7.82[a]	−2.16[b]	−9.80[a]	−2.52[b]
	I	−6.43[c]	−5.40	−8.78	−3.66
	V	−7.74	−2.16	−9.80	−2.65
	VI	−7.82	−4.59	−9.13	−2.52
	DFG-out *binders*	−6.66[a]	−2.81[b]	−12.4[a]	−3.67[b]
	II	−6.13	−3.71	−9.20	−3.67
	III	−5.36	−3.74	−12.4[c]	−11.12
	VII	−6.66	−3.12	−10.44	−4.64
	Dual conformation binders	−5.58[a]	−2.39[b]	−10.24[a]	−4.69[b]
	IV	−5.58[c]	−2.39	−10.24[c]	−4.69
GOLD	DFG-in *binders*	79.72[a]	42.04[b]	89.61[a]	35.02[b]
	I	55.34[c]	42.04	56.12	45.03
	V	79.72	53.09	89.61	61.40
	VI	60.26	45.81	58.61[c]	35.02
	DFG-out *binders*	76.10[a]	47.52[b]	95.84[a]	45.74[b]
	II	71.26[c]	51.20	78.76[c]	54.44
	III	76.10[c]	56.65	95.84	87.32
	VII	65.79	47.52	71.45	45.74
	Dual conformation binders	64.78[a]	49.06[b]	74.17[a]	55.84[b]
	IV	64.78[c]	49.06[c]	74.17	55.84

The roman numerals denote the name of the dataset (Fig. S6) used for testing.
[a] Highest score among all compounds of the dataset.
[b] Lowest score among all compounds of the dataset.
[c] Most active compound of dataset is also the highest scorer of the same dataset.

6. Virtual screening

Virtual screening was done using the fourth dataset of 10^7 compounds to identify potential allosteric fragments to form the tail part of the designed leads. The compounds of the dataset with a Tanimoto similarity co-efficient of >0.5 to more than two of the existing sub-structures were removed in order to ensure identification of sub-structures different from the ones comprising the existing sub-structure set. The 8 million compounds thus retained were further clustered using maximum dissimilarity clustering algorithm into four clusters of 2 million compounds each [63–65]. From each of the individual four clusters, 2.5 lakhs most distant compounds from the cluster centre were selected. Thus, a total of 1 million diverse compounds were extracted from the dataset of 10^7 compounds for virtual screening. These 1 million compounds were subjected to virtual screening using two protocols GOLD and Glide with one representative DFG-in (1A9U) and DFG-out (1KV2) conformations of p38 MAPK. Ten poses were generated for each of the 1 million compound of the dataset. From this, only the best scoring pose of each compound was selected for evaluation.

The designed docking-score filter was now applied on the score components of the best scored poses of both the docking protocols. Score components of both the docking protocols were compared individually with the docking-score filter. Only those compounds satisfying all the 8 thresholds for DFG-in and DFG-out individually were retained (Table S14). T1 (vdW), T5 (hb_ext), T7 (vdW_ext) are observed to be highly efficient individually to filter out inactives with a high average attrition rate of 96%. Analysis of the performance of the designed docking filters reconfirms the role of vdW and H-bond interactions in the binding and selectivity of p38 MAPK inhibitors. The present analysis reflects attrition from 10^6 to 10^3 using docking filters. The docking filters filtered out 985,373 DFG-in and 899,888 DFG-out compounds retaining the 14,727 DFG-in and 10, 243 DFG-out compounds satisfying all the docking thresholds (Fig. 6). These set of hits were used for analysis using sub-structure interaction filters. The number of database compounds satisfying the DFG-in thresholds of virtual screening filters were found to be more in number than those satisfying the DFG-out criterion. The reason for this can be attributed to the fact that present-day databases contain molecules having smaller scaffolds that bind well to the DFG-in site which is also smaller in size like the active site of other proteins. However, the DFG-out active site region is comparatively larger leading to the rejection of small molecules based on their sub-optimal binding. 100 hits comprising of 75 organic synthetic molecules, 5 natural products and 20 drugs were selected based on their occupancy and interactions with different regions of p38 MAPK active site (Table S15).

7. Fragment library generation and lead design

The binding modes and interactions of the 100 virtual screening hits were used to mark out fragments with a potential to be a part of the type II lead. The hundred virtual screening hits were pruned into fragments based on their interactions with different

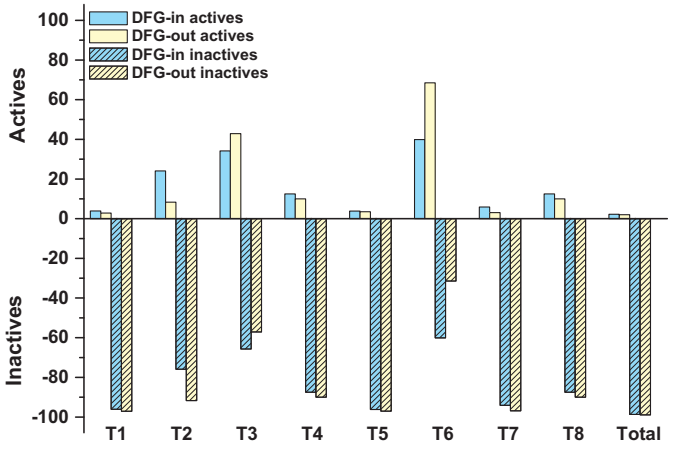

Fig. 6. Analysis of the performance of the designed docking filters on a database of 106 compounds for DFG-in and DFG-out conformations of p38 MAP kinase. The figure depicts the percent actives (following threshold) and inactives (not following threshold) obtained for each threshold individually and as a sum using the designed docking filters. T1–T8 represents the 8 individual thresholds (T1: vdW; T2: Coul; T3: Lipo; T4: Gscore; T5: S(hb_ext); T6: S(int); T7: S(vdW_ext); and T8: Fitness) and total stands for compounds following all 8 thresholds.

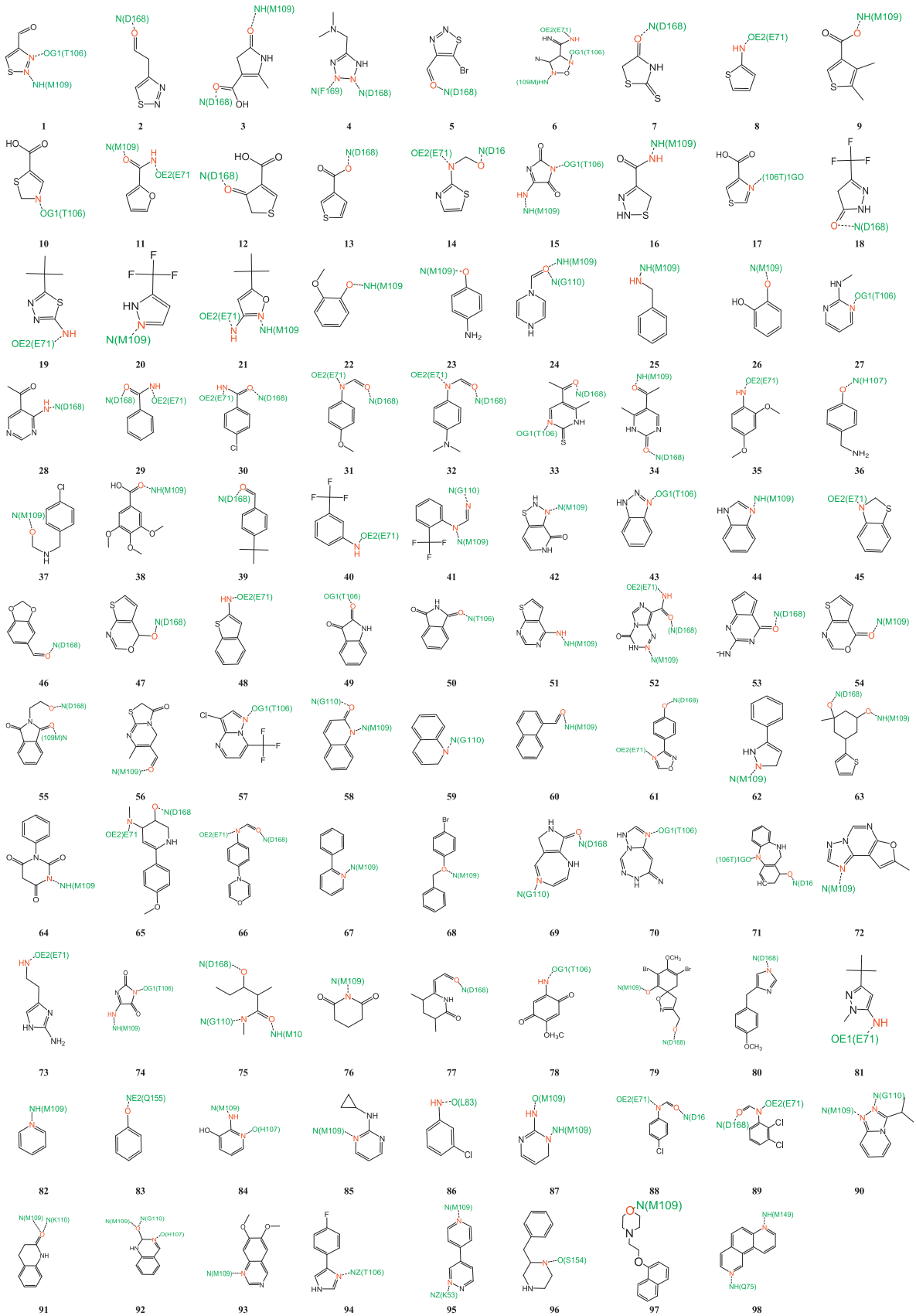

Fig. 7. New p38 MAP kinase sub-structure library designed from the allosteric fragments extracted from the 100 virtual screening hits.

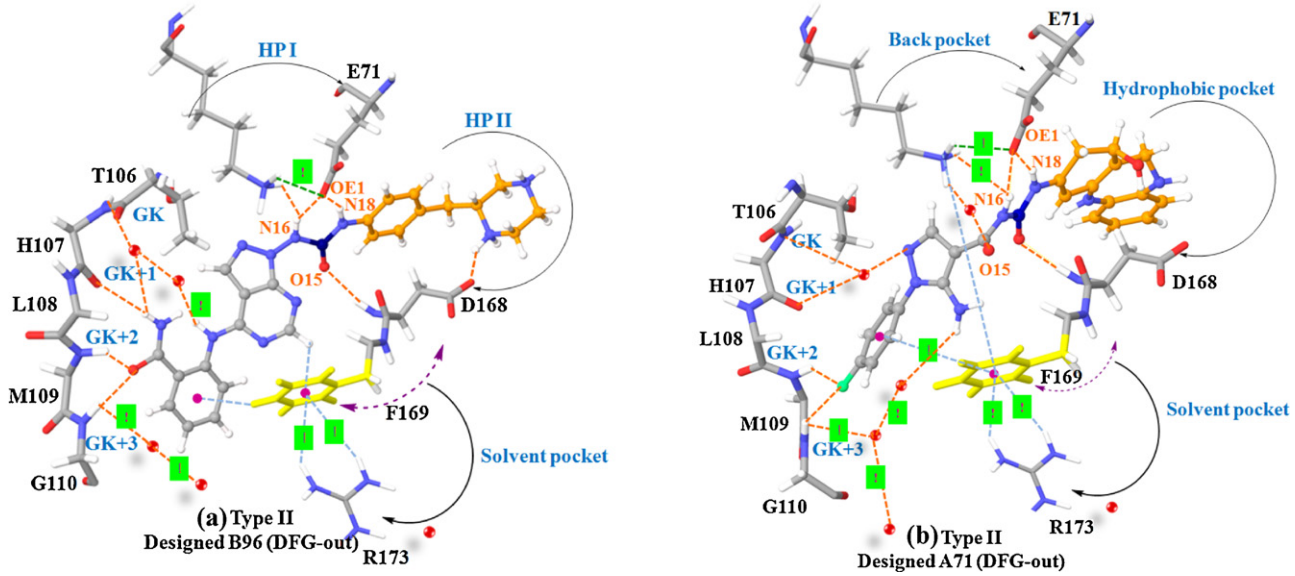

Fig. 8. The figure depicts the conformational variation in DFG-loop and corresponding active-site residues along with H-bond and non-covalent interaction framework of the two top ranked designed inhibitors from ensemble docking A71, B96 with p38 MAP kinase as observed during the 10 ns molecular dynamics simulation.

regions of active site in order to extract the allosteric site fragments (Fig. S7). The 98 prioritized, allosteric site interacting fragments extracted from the 100 virtual screening hits were used to formulate the fragment library (Fig. 7). The 2D and 3D descriptors of all sub-structures were calculated and the fingerprints in PubChem format were generated [66,67]. The integration of complexity of data is ensured by retention of 2D and 3D properties along with interaction of the sub-structures. The fragment library generated in this manner can be a good starting point to design novel leads using FBDD. These prioritized fragments were used to design p38 MAPK leads.

The existing type I inhibitors bind to the conserved ATP binding site when the catalytic kinase domain is in an active conformation and the conserved DFG-loop at the beginning of the activation loop is in the "in "conformation. A number of crystal structures reveal the inactive conformations of kinase where the DFG-loop is in either the "in" or "out" conformation. In the DFG-out conformation, the aspartate of the DFG-loop points to the back cleft of the ATP site and the phenylalanine extends into the ATP binding site. The DFG-loop backbone is also shifted into the ATP binding site thereby opening up a non-conserved hydrophobic pocket which is exploited by type II inhibitors [68,69]. Type II leads were designed for the DFG-out conformation of kinase by engineering the existing type I inhibitors with allosteric fragments extracted from the virtual screening hits. The leads were designed by merging three parts namely head, tail and linker. The head is an ATP site binder with an inclination to form H-bonds with amino acid residues of the hinge region and hydrophobic interactions with the adenine region of the ATP binding site. A short urea linker is used as a hook to join the head and allosteric site fragments. The tail comprises of allosteric fragments with an H-bond donor–acceptor pair and a hydrophobic motif to bind exclusively to the allosteric site of p38 MAPK. Based on this blue-print, new type II p38 MAPK leads were designed using the 39 existing type I binders as head, a urea linker and the 98 allosteric site fragments extract from the 100 virtual screening hits as tail. This gave a huge combinatorial library of 3822 leads. Based on our interests, we sorted out 196 leads comprising of two ATP binders (2BAL_PQA, 3CG2_N4D) along with urea linker and the 98 allosteric site fragments (Fig. S8).

7.1. Evaluation of designed leads

Kinase inhibitors on binding are known to cause small local movement of side chains to large domain shifts leading to receptor rearrangement. Increase in receptor flexibility is therefore required to capture this induced-fit nature. Considering the high computational time required for MD and the complications associated with flexible docking, ensemble docking with eight p38 MAPK crystal structures exclusively in DFG-out conformation was opted initially. Regular rigid docking using Glide was followed by the induced fit docking (IFD) of Schrodinger in an attempt to incorporate protein flexibility. The two top ranked designed leads B96, A71 were further subjected to a MD simulation of 40 ns in order to test the designed leads over a large conformational space.

The docked poses and MD simulation trajectory of the designed leads on visualization show that the individual fragments constructing the new leads recap similar pattern of interactions and maintain their original binding modes. The ATP site binder occupies the adenine region and the gatekeeper residue back-pocket whereas the allosteric fragment occupies the hydrophobic pocket opened up on the flipping of F169. The urea linker positively interacts with D168 of DFG-loop and the conserved E71 in all time-frames (Fig. 8). The H-bond network formed by the major interacting motifs like gatekeeper, DFG-loop, hinge, conserved E71 and K53 are intact during the MD simulation (Figs. S9 and S10). The conserved H-bonds with hinge as displayed by the known type I is also maintained throughout the simulation by both the designed inhibitors. The gatekeeper residue T106 due to its small size participates less frequently in H-bond network however the back-pocket residues lining the gatekeeper form H-bond with the pyrazolidine nitrogen through bridging water during the time-scale of 8.5–9.5 ns and 15.8–16.2 ns where major fluctuations are observed in the T106. The OE1 of the conserved E71 consistently forms H-bonds with the two linker nitrogen (N16, N18). The cationic head of K53, the salt-bridge former exhibits H-bonds with oxygen (O15) lying at the posterior end of ATP fragment and one of the linker nitrogen (N16). However, the cationic head of K53 forms cation–π interactions with the F169 of the DFG-loop only when the average distance is in the range of 3.125 ± 1 Å in the time-scale of 3.0–5.0

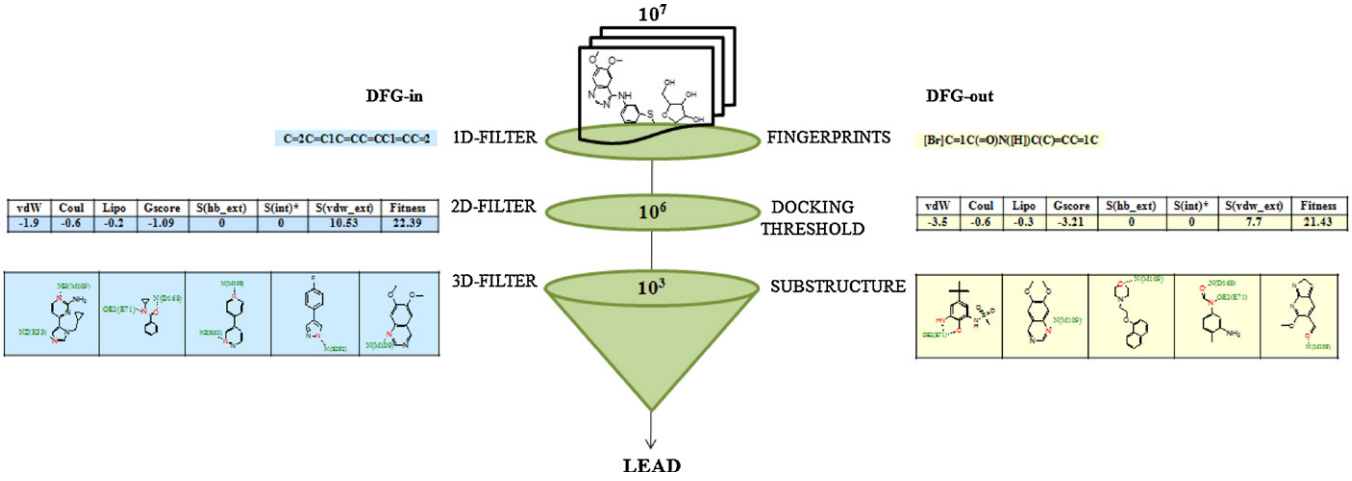

Fig. 9. Overview of the target specific filters developed for p38 MAP kinase based on the docking analysis of 138 co-crystal interactions with 98 crystal structures from PDB. The docking filter is an outcome of the evaluation of docking protocols Glide 4.5 and GOLD 3.2 for DFG-in and DFG-out conformation of p38 MAP kinase. Binding modes and chemotype selectivity delineated by docking during evaluation was used for the construction of target specific sub-structure library. The sub-structure filters are the sub-structure based pharmacophore representatives which were also converted to PubChem Fingerprints and SMILES. Same logic has been applied to design each of this filters for DFG-in and DFG-out conformations separately.

and 18.0–20.0 ns, as the distance between the two residues is varying. The side-chain of F169 shows a tendency to form cation–π interactions with positively charged residues. These interactions increase the potential of the F169 aromatic ring to be solvated. Majority of the water molecules are observed to mediate interactions between active site residues (K53, V105, H107, G110, D112, G170, S154, R173, etc.) and ligand. These bridging waters are seen to render stability to the active site in the presence of flexible kinase domains. The main contributions of water to the specificity and the affinity of ligand binding are characterized by their role in networking H-bonds. The amide moiety of D168 unfailingly interacts with the oxygen of linker. The DFG-loop interactions vary considerably in the time-scale of 8.3–9.0 ns and 24.0–28.0 ns which are controlled by the orientation of F169. The aromatic-ring of F169 interacts with the heterocyclic head of the inhibitor through π-stacking. The active site of p38 MAP kinase has an aromatic-network comprising of eight residues namely W18, Y35, Y69, Y103, Y140, F169, Y323 and F327. Y35 and F169 are the only aromatic amino acids which form direct contact with the inhibitor during the MD simulation. The analysis of frames clustered for these time-scales with respect to others reveal that major transitions occur in the activation-loop, F169 and K53 which in turn influence the surrounding residues. The designed leads were thus evaluated in silico on the basis of occupancy of active site, binding mode and interactions.

8. Conclusions

Achieving specificity is a problem of outstanding importance for kinases in general and p38 MAPK in particular owing to its key therapeutic potential. The drug–receptor interactions play pivotal role in inhibition as evidenced through molecular dynamics simulations deciphering the role of interaction-network in inhibitor binding. In addition, the chemotype in kinase inhibitors was observed to display specificity for a particular region of binding site. This emphasizes the use of target specific fragments for the design of kinase leads. The efficacy of the existing type I and the low availability of type II necessitate virtual screening of allosteric fragments. Docking has always been the most used tool for virtual screening however with an unvarying requirement for a target specific filter. Therefore the current work focuses the development and application of virtual screening filters based on docking-score and sub-structure interactions to identify allosteric fragments for the design of type II p38 MAP kinase leads (Fig. 9). The filters on testing display their capacity to identify target specific compounds. The use of these two virtual screening filters in the virtual screening of the 10 million compounds gave 100 hits with 98 fragments displaying a tendency to bind to the allosteric pocket. This validates the capacity and use of such filters in virtual screening. The fragment library generated from the allosteric site fragments extracted from the virtual screening hits were used for reengineering existing type I inhibitors to type II. The designed inhibitors maintain the binding modes and spatial orientations to the same active site region as their source fragments even on spanning a relatively large conformational space during ensemble docking and MD. The fragment tailoring approach involving the growing of existing type I binders with allosteric site fragments from virtual screening hits for the DFG-out conformation of kinase is a novel way to identify target-specific fragments and obtain diverse type II leads. Thus, a set of rationally designed compounds can be provided for assaying rather than the use of huge libraries of compounds. The current strategy used for the development of target-specific virtual screening filters can be easily extendable to other kinases.

Acknowledgement

Department of Science and Technology, New Delhi is thanked for Swarnajayanti Fellowship to GNS and Women Scientist Fellowship to PB. DBT and CSIR, New Delhi are also thanked for financial assistance.

Appendix A. Supplementary data

Supplementary data associated with this article can be found, in the online version, at doi:10.1016/j.jmgm.2011.12.009.

References

[1] R.G. Kulkarni, G. Achaiah, G.N. Sastry, Novel targets for anti-inflammatory and anti-arthritic agents, Curr. Pharm. Des. 12 (2006) 2437–2454.
[2] M.E.M. Noble, J. Endicott, L.K. Johnson, Protein kinase inhibitors: insights into drug design from structure, Science 303 (2004) 1800–1805.
[3] M. Huse, J. Kuriyan, The conformational plasticity of protein kinases, Cell 109 (2002) 275–282.
[4] L.A. Smyth, I. Collins, Measuring and interpreting the selectivity of protein kinase inhibitors, J. Chem. Biol. 2 (2009) 31–151.
[5] R. Morphy, Selectively nonselective kinase inhibition: striking the right balance, J. Med. Chem. 53 (2010) 1413–1437.

[6] F. Zuccotto, E. Ardini, E. Casale, M. Angiolini, Through the "Gatekeeper door": exploiting the active kinase conformation, J. Med. Chem. 53 (2010) 2681–2694.
[7] I. Collins, P. Workman, Design and development of signal transduction inhibitors for cancer treatment: experience and challenges with kinase targets, Curr. Signal Transduct. Ther. 1 (2006) 13–23.
[8] Y. Shana, M.A. Seeligerb, M.P. Eastwooda, F. Frankb, H. Xua, M. Jensena, R.O. Drora, J. Kuriyanb, D.E. Shaw, A conserved protonation-dependent switch controls drug binding in the Abl kinase, Proc. Natl. Acad. Sci. U.S.A. 106 (2009) 139–144.
[9] D. Huang, T. Zhou, K. Lafleur, C. Nevado, A. Caflisch, Kinase selectivity potential for inhibitors targeting the ATP binding site: a network analysis, Bioinformatics 26 (2010) 198–204.
[10] R. Soliva, J.L. Gelpi, C. Almansa, M. Virgili, M. Orozco, Dissection of the recognition properties of p38 MAP kinase determination of the binding mode of a new pyridinyl-heterocycle inhibitor family, J. Med. Chem. 50 (2007) 283–293.
[11] J.J. Sutherland, R.E. Higgs, I. Watson, M. Vieth, Chemical fragments as foundations for understanding target space and activity prediction, J. Med. Chem. 51 (2008) 2689–2700.
[12] C. Pargellis, L. Tong, L. Churchill, P.F. Cirillo, T. Gilmore, A.G. Graham, P.M. Grob, E.R. Hickey, N. Moss, S. Pav, J. Regan, Inhibition of p38 MAP kinase by utilizing a novel allosteric binding site, Nat. Struct. Biol. 9 (2002) 268–272.
[13] A.K. Ghose, T. Herbertz, D.A. Pippin, J.M. Salvino, J.P. Mallamo, Knowledge based prediction of ligand binding modes and rational inhibitor design for kinase drug discovery, J. Med. Chem. 51 (2008) 5149–5171.
[14] P. Badrinarayan, G.N. Sastry, Sequence structure, and active site analyses of p38 MAP kinase: exploiting DFG-out conformation as a strategy to design new type II leads, J. Chem. Inf. Model. 51 (2011) 115–129.
[15] S.V. Shelke, B. Cutting, X. Jiang, B.H. Koliwer, D.S. Strasser, O. Schwardt, S. Kelm, B. Ernst, A fragment-based in situ combinatorial approach to identify high-affinity ligands for unknown binding sites, Angew. Chem. Int. Ed. 49 (2010) 5721–5725.
[16] A.S. Reddy, S.P. Pati, P.P. Kumar, H.N. Pradeep, G.N. Sastry, Virtual screening in drug discovery—a computational perspective, Curr. Protein Pept. Sci. 8 (2007) 329–351.
[17] P. Badrinarayan, G.N. Sastry, Virtual high-throughput screening in new lead identification, Comb. Chem. High Throughput Screen. 14 (2011) 840–860.
[18] V. Zoete, A. Grosdidier, O. Michielin, Docking virtual high throughput screening and in silico fragment-based drug design, J. Cell Mol. Med. 13 (2009) 238–248.
[19] M. Stahl, M. Rarey, Detailed analysis of scoring functions for virtual screening, J. Med. Chem. 44 (2001) 1035–1042.
[20] E. Perola, W.P. Walters, P.S. Charifson, A detailed comparison of current docking and scoring methods on systems of pharmaceutical relevance, Proteins Struct. Funct. Bioinf. 56 (2004) 235–249.
[21] S.M. Vogel, M.R. Bauer, F.M. Boeckler, DEKOIS: demanding evaluation kits for objective in silico screening—a versatile tool for benchmarking docking programs and scoring functions, J. Chem. Inf. Model. 51 (2011) 2650–2665.
[22] S.G. Rohrer, K. Baumann, Maximum unbiased validation (MUV) data sets for virtual screening based on PubChem bioactivity data, J. Chem. Inf. Model. 49 (2009) 169–184.
[23] B. Musafia, H. Senderowitz, Bioactive conformational biasing: a new method for focusing conformational ensembles on bioactive-like conformers, J. Chem. Inf. Model. 49 (2009) 2469–2480.
[24] W. Sherman, H.S. Beard, R. Farid, Use of an induced fit receptor structure in virtual screening, Chem. Biol. Drug Des. 67 (2006) 83–84.
[25] M. Brylinski, J. Skolnick, Comprehensive structural and functional characterization of the human kinome by protein structure modeling and ligand virtual screening, J. Chem. Inf. Model. 50 (2010) 1839–1854.
[26] R.G. Kulkarni, P. Srivani, G. Achaiah, G.N. Sastry, Strategies to design of pyrazolyl urea derivatives for p38 kinase inhibition: a molecular modeling study, J. Comput. Aided Mol. Des. 25 (2007) 155–166.
[27] P. Badrinarayan, P. Srivani, G.N. Sastry, Design of 1-arylsulfamido-2-alkylpiperazine derivatives as secreted PLA2 inhibitors, J. Mol. Model. 17 (2011) 817–831.
[28] P. Srivani, D. Usharani, E.D. Jemmis, G.N. Sastry, Subtype selectivity in phosphodiesterase 4 (PDE4): a bottleneck in rational drug design, Curr. Pharm. Des. 14 (2008) 3854–3872.
[29] R.G. Kulkarni, G. Achaiah, G.N. Sastry, Molecular modeling studies of phenoxypyrimidinyl imidazoles as p38 kinase inhibitors using QSAR and docking, Eur. J. Med. Chem. 43 (2008) 830–838.
[30] M. Chourasia, G.M. Sastry, G.N. Sastry, Proton binding sites and conformational analysis of H^+K^+-ATPase, Biochem. Biophys. Res. Commun. 336 (2005) 961–966.
[31] P. Srivani, G.N. Sastry, Potential choline kinase inhibitors: a molecular modeling study of bis-quinolinium compounds, J. Mol. Graphics Modell. 27 (2009) 676–688.
[32] P. Srivani, E. Srinivas, R. Raghu, G.N. Sastry, Molecular modeling studies of pyridopurinone derivatives—potential phosphodiesterase5 inhibitors, J. Mol. Graphics Modell. 26 (2008) 378–390.
[33] H.M. Berman, J. Westbrook, Z. Feng, G. Gilliland, T.N. Bhat, H. Weissig, I.N. Shindyalov, P.E. Bourne, The protein data bank, Nucleic Acids Res. 28 (2000) 235–242.
[34] W. Lumeras, F. Caturla, L. Vidal, C. Esteve, C. Balagu, A. Orellana, M. Dominguez, R. Roca, J.M. Huerta, N. Godessart, B. Vidal, Design, synthesis, and structure–activity relationships of aminopyridine N-oxides, a novel scaffold for the potent and selective inhibition of p38 mitogen activated protein kinase, J. Med. Chem. 52 (2009) 5531–5545.
[35] S.T. Wrobleski, S. Lin, J. Hynes, H. Wu, S. Pitt, D.R. Shen, R. Zhang, K.M. Gillooly, D.J. Shuster, K.W. McIntyre, A.M. Doweyko, K.F. Kish, J.A. Tredup, G.J. Duke, J.S. Sack, M. McKinnon, J. Dodd, J.C. Barrish, G.L. Schieven, K. Leftheris, Synthesis and SAR of new pyrrolo[2,1-f][1,2,4]triazines as potent p38a MAP kinase inhibitors, Bioorg. Med. Chem. Lett. 18 (2008) 2739–2744.
[36] A.G. Montalban, E. Boman, C.D. Chang, S.C. Ceide, R. Dahl, D. Dalesandro, N.G.J. Delaet, E. Erb, J.T. Ernst, A. Gibbs, J. Kahl, L. Kessler, J. Lundstrom, S. Miller, H. Nakanishi, E. Roberts, E. Saiah, R. Sullivan, Z. Wang, C.J. Larson, The design and synthesis of novel α-ketoamide-based p38 MAP kinase inhibitors, Bioorg. Med. Chem. Lett. 18 (2008) 1772–1777.
[37] R.M. Angell, T.D. Angell, P. Bamborough, M.J. Bamford, C. Chung, S.G. Cockerill, S.S. Flack, K.L. Jones, D.I. Laine, T. Longstaff, S. Ludbrook, R. Pearson, K.J. Smith, P.A. Smee, D.O. Somers, A.L. Walker, Biphenyl amide p38 kinase inhibitors 4: DFG-in and DFG-out binding modes, Bioorg. Med. Chem. Lett. 18 (2008) 4433–4437.
[38] S.A. Laufer, D.R.J. Hauser, D.M. Domeyer, K. Kinkel, A.J. Liedtke, Design, synthesis, and biological evaluation of novel tri- and tetrasubstituted imidazoles as highly potent and specific ATP-mimetic inhibitors of p38 MAP kinase: focus on optimized interactions with the enzyme's surface-exposed front region, J. Med. Chem. 51 (2008) 4122–4149.
[39] T.G.M. Dhar, S.T. Wrobleski, S. Lin, J.A. Furch, D.S. Nirschl, Y. Fan, G. Todderud, S. Pitt, A.M. Doweyko, J.S. Sack, A. Mathur, M. McKinnon, J.C. Barrish, J.H. Dodd, G.L. Schieven, K. Leftheris, Synthesis and SAR of p38a MAP kinase inhibitors based on heterobicyclic scaffolds, Bioorg. Med. Chem. Lett. 17 (2007) 5019–5024.
[40] J.G. Cumming, C.L. McKenzie, S.G. Bowden, D. Campbell, D.J. Masters, J. Breed, P.J. Jewsbury, Novel, potent and selective anilinoquinazoline and anilinopyrimidine inhibitors of p38 MAP kinase, Bioorg. Med. Chem. Lett. 14 (2004) 5389–5394.
[41] J.J. Irwin, B.K. Shoichet, ZINC – a free database of commercially available compounds for virtual screening, J. Chem. Inf. Model. 45 (2005) 177–182.
[42] L.C. Blum, J.L. Reymond, 970 million druglike small molecules for virtual screening in the chemical universe database GDB-13, J. Am. Chem. Soc. 131 (2009) 8732–8733.
[43] L.O. Haustedt, C. Mang, K. Siems, H. Schiewe, Rational approaches to natural-product-based drug design, Curr. Opin. Drug Discov. Dev. 9 (2006) 445–462.
[44] C.A. Lipinski, F. Lombardo, B.W. Dominy, P.J. Feeney, Experimental and computational approaches to estimate solubility and permeability in drug discovery and development settings, Adv. Drug Deliv. Rev. 46 (2001) 3–26.
[45] K. Zhu, M.R. Shirts, R.A. Friesner, Improved methods for side chain and loop predictions via the protein local optimization program: variable dielectric model for implicitly improving the treatment of polarization effects, J. Chem. Theory Comput. 3 (2007) 2108–2119.
[46] M.A. Eswar, M. Renom, B. Webb, M.S. Madhusudhan, D. Eramian, M. Shen, U. Pieper, A. Sali, Comparative protein structure modeling with MODELLER, Curr. Protoc. Bioinf. 15 (2006) 5.6.1–5.6.30.
[47] S.C. Lovell, I.W. Davis, W.B. Arendall III, P.I.W. Bakker, J.M. Word, M.G. Prisant, J.S. Richardson, D.C. Richardson, Structure validation by Cα geometry: phi, psi and Cbeta deviation, Proteins Struct. Funct. Genet. 50 (2003) 437–450.
[48] M. Wiederstein, M.J. Sippl, ProSA-web: interactive web service for the recognition of errors in three-dimensional structures of proteins, Nucleic Acids Res. 35 (2007) W407–W410.
[49] M. Heinig, D. Frishman, STRIDE: a web server for secondary structure assignment from known atomic coordinates of proteins, Nucleic Acids Res. 32 (2004) W500–W502.
[50] M. Rarey, B. Kramer, T. Lengauer, G. Klebe, A fast flexible docking method using an incremental construction algorithm, J. Mol. Biol. 261 (1996) 470–489.
[51] R.A. Friesner, J.L. Banks, R.B. Murphy, T.A. Halgren, J.J. Klicic, D.T. Mainz, M.P. Repasky, E.H. Knoll, M. Shelley, J.K. Perry, D.E. Shaw, P. Francis, P.S. Shenkin, Glide: a new approach for rapid accurate docking and scoring. 1. Method and assessment of docking accuracy, J. Med. Chem. 47 (2004) 1739–1749.
[52] G. Jones, P. Willett, R.C. Glen, A.R. Leach, R. Taylor, Development and validation of a genetic algorithm for flexible docking, J. Mol. Biol. 267 (1997) 727–748.
[53] G. Wu, D.H. Robertson, C.L. Brooks III, M. Vieth, Detailed analysis of grid-based molecular docking: a case study of CDOCKER-CHARMM-based MD docking algorithm, J. Comp. Chem. 24 (2003) 1549–1562.
[54] K.S. Watts, P. Dalal, R.B. Murphy, W. Sherman, R.A. Friesner, J.C. Shelley, ConfGen: a conformational search method for efficient generation of bioactive conformers, J. Chem. Inf. Model. 50 (2010) 534–546.
[55] Z. Guo, U. Mohanty, J. Noehre, T.K. Sawyer, W. Sherman, G. Krilov, Probing the α-helical structural stability of stapled p53 peptides: molecular dynamics simulations and analysis, Chem. Biol. Drug Des. 75 (2010) 348–359.
[56] K.J. Bowers, E. Chow, H. Xu, R.O. Dror, M.P. Eastwood, B.A. Gregersen, J.L. Klepeis, I. Kolossvary, M.A. Moraes, F.D. Sacerdoti, J.K. Salmon, Y. Shan, D.E. Shaw, Scalable algorithms for MD simulations on commodity clusters, in: Proceedings of the ACM/IEEE Conference on Supercomputing (SC06), November 11–17, Tampa, FL, 2006.
[57] D.B. Kitchen, H. Decornez, J.R. Furr, J. Bajorath, Docking and scoring in virtual screening for drug discovery: methods and applications, Nat. Rev. Drug Discov. 3 (2004) 935–949.
[58] Z. Deng, C. Chuaqui, J. Singh, Structural interaction fingerprint (SIFt): a novel method for analyzing three-dimensional protein–ligand binding interactions, J. Med. Chem. 47 (2004) 337–344.
[59] C. Chuaqui, Z. Deng, J. Singh, Interaction profiles of protein kinase–inhibitor complexes and their application to virtual screening, J. Med. Chem. 48 (2005) 121–133.

[60] S.F. Altschul, W. Gish, W. Miller, E.W. Myers, D.J. Lipman, Basic local alignment search tool, J. Mol. Biol. 215 (1990) 403–410.
[61] J.D. Thompson, D.G. Higgins, T.J. Gibson, CLUSTALW: improving the sensitivity of progressive multiple sequence alignment through sequence weighting position-specific gap penalties and weight matrix choice, Nucleic Acids Res. 22 (1994) 4673–4680.
[62] J. Felsenstein, PHYLIP-phylogeny inference package (version 3.2), Cladistics 5 (1989) 164–166.
[63] M. Hassan, J.P. Bielawski, J.C. Hempel, M. Waldman, Optimization and visualization of molecular diversity of combinatorial libraries, Mol. Divers. 2 (1996) 64–74.
[64] Y. Cao, T. Jiang, T. Girke, Accelerated similarity searching and clustering of large compound sets by geometric embedding and locality sensitive hashing, Bioinformatics 26 (2010) 953–959.
[65] D. Weininger, A. Weininger, J.L. Weininger, SMILES. 2. Algorithm for generation of unique SMILES notation, J. Chem. Inf. Model. 29 (1989) 97–101.
[66] C.W. Yap, PaDEL-Descriptor: an open source software to calculate molecular descriptors and fingerprints, J. Comput. Chem. 32 (2011) 1466–1474.
[67] Y. Wang, J. Xiao, T.O. Suzek, J. Zhang, J. Wang, S.H. Bryant, PubChem: a public information system for analyzing bioactivities of small molecules, Nucleic Acids Res. 37 (2009) W623–W633.
[68] M. Vogtherr, K. Saxena, S. Hoelder, S. Grimme, M. Betz, U. Schieborr, B. Pescatore, M. Robin, L. Delarbre, T. Langer, K.U. Wendt, H. Schwalbe, NMR characterization of kinase p38 dynamics in free and ligand-bound forms, Angew. Chem. Int. Ed. 45 (2006) 993–997.
[69] F. Filomia, F.D. Rienzo, M.C. Menziani, Insights into MAPK p38a DFG flip mechanism by accelerated molecular dynamics, Bioorg. Med. Chem. 18 (2010) 6805–6812.